THE ASTROPHYSICAL JOURNAL, 493:351–367, 1998 January 20

FORMATION OF LOW-MASS X-RAY BINARIES. II. COMMON ENVELOPE EVOLUTION OF PRIMORDIAL BINARIES WITH EXTREME MASS RATIOS

VASSILIKI KALOGERA[1] AND RONALD F. WEBBINK
Astronomy Department, University of Illinois at Urbana-Champaign, 1002 West Green Street, Urbana, IL 61801;
vicky@astro.uiuc.edu, webbink@astro.uiuc.edu
Received 1996 February 26; accepted 1997 August 27

ABSTRACT

We study the formation of low-mass X-ray binaries (LMXBs) through helium star supernovae in binary systems that have each emerged from a common envelope phase. LMXB progenitors must satisfy a large number of evolutionary and structural constraints, including survival through common envelope evolution, through the post–common envelope phase, where the precursor of the neutron star becomes a Wolf-Rayet star, and survival through the supernova event. Furthermore, the binaries that survive the explosion must reach interaction within a Hubble time and must satisfy stability criteria for mass transfer. These constraints, imposed under the assumption of a symmetric supernova explosion, prohibit the formation of short-period LMXBs transferring mass at sub-Eddington rates through *any* channel in which the intermediate progenitor of the neutron star is not completely degenerate. Barring accretion-induced collapse, the existence of such systems therefore requires that natal kicks be imparted to neutron stars.

We use an analytical method to synthesize the distribution of nascent LMXBs over donor masses and orbital periods and evaluate their birthrate and systemic velocity dispersion. Within the limitations imposed by observational incompleteness and selection effects, and our neglect of secular evolution in the LMXB state, we compare our results with observations. However, our principal objective is to evaluate how basic model parameters (common envelope ejection efficiency, rms kick velocity, primordial mass ratio distribution) influence these results. We conclude that the characteristics of newborn LMXBs are primarily determined by age and stability constraints and the efficiency of magnetic braking and are largely independent of the primordial binary population and the evolutionary history of LMXB progenitors (except for extreme values of the average kick magnitude or of the common envelope ejection efficiency). Theoretical estimates of total LMXB birthrates are not credible, since they strongly depend on the observationally indeterminate frequency of primordial binaries with extreme mass ratios in long-period orbits.

Subject headings: binaries: close — stars: evolution — stars: interiors — stars: neutron — X-rays: stars

1. INTRODUCTION

The existence of low-mass X-ray binaries (LMXBs) poses critical questions to the theories for the evolution of close binaries. They are believed to be accreting neutron stars or possibly black holes with low-mass companions (for recent reviews, see Bhattacharya & van den Heuvel 1991; Verbunt 1993). The major problem concerning their origin is that their orbits are now so small that they could not accommodate the advanced evolution of the progenitor of the compact object. A similar question was originally posed for cataclysmic binaries, and a solution was suggested by Paczyński (1976): a common envelope is formed around the binary, and the spiral-in of the secondary into the primary causes the envelope to be ejected and the orbit to contract substantially while exposing the degenerate core of the primary as a newly formed white dwarf. A common envelope phase is adequate to solve the puzzle of LMXBs, as well, since it can not only account for the shrinkage of the orbit, but it also reduces the primary mass, so that the disruptive effect of mass loss at supernova is weakened, increasing the chance for survival of LMXB progenitors.

Several scenarios have been proposed for the formation of LMXBs in the galactic disk, and three out of four invoke a common envelope phase. One involves accretion-induced collapse (AIC) of an accreting white dwarf. The process was first discussed by Whelan & Iben (1973), although in a context other than LMXB formation. A second scenario proposes that a massive helium core, exposed in a small orbit by spiral-in evolution, collapses to form a neutron star or a black hole (van den Heuvel 1983). A variant of this evolutionary path, involving extensive wind mass loss in place of common envelope evolution, has been suggested (Romani 1992) as an avenue for producing black hole LMXBs. More recently, triple-star evolution has been put forward for LMXB formation with either a black hole or a neutron star and involves the formation of a Thorne-Żytkow star by merger of a massive X-ray binary and engulfment of the third component in a common envelope phase (Eggleton & Verbunt 1986). A fourth scenario has been proposed, the direct-supernova mechanism (Kalogera 1998), which obviates the need for a common envelope phase and relies solely on natal kicks imparted to neutron stars to keep the systems bound and also decrease the orbital separation.

All of these scenarios present plausible formation channels for LMXBs. However, quantitative analysis of these evolutionary channels has been hampered by our limited understanding of the details of the various physical processes involved (e.g., spiral-in process, Wolf-Rayet mass loss, and asymmetric supernova explosion). It is possible to tailor an evolutionary model to reproduce the properties of an isolated LMXB, but this exercise provides little per-

[1] Present address: Harvard-Smithsonian Center for Astrophysics, 60 Garden Street, MS 51, Cambridge, MA 02138; e-mail: vkalogera@cfa.harvard.edu.

spective on whether the putative initial conditions and subsequent tailoring are plausible. A more useful approach is to model the evolution of an entire ensemble of primordial binaries under a common set of assumptions and to analyze the statistical properties of the LMXB population. Such an approach has been taken in the past for the study of other binary populations (see, e.g., Lipunov & Postnov 1988; de Kool 1992; Kolb 1993; Tutukov & Yungel'son 1993; Politano 1996) and more recently for LMXBs (Romani 1992; Iben, Tutukov, & Yungel'son 1995; Terman, Taam, & Savage 1996).

Our purpose here is to model the evolution of a primordial binary population through a sequence of stages involving, among others, a common envelope phase and the supernova explosion of a helium star, and leading to the formation of LMXBs. Although a direct result of our calculations is the birth frequency of LMXBs, we focus more on identifying the properties of LMXB progenitors and on investigating the dependence of the final population characteristics on the uncertain model parameters. We also examine the possibility of comparing our results to observations and constraining the observationally undetermined properties of primordial binaries feeding LMXB formation. Although we study one evolutionary channel here, our techniques can be straightforwardly applied to other channels, and some of our conclusions hold for all the LMXB formation paths that invoke a common envelope phase.

In § 2 the evolutionary scenario is described in some detail. The relevant constraints that binaries must satisfy at various instances throughout their evolution and the resulting limits on the LMXB progenitor parameter space are identified in § 3. We find that asymmetric supernova explosions are needed to explain LMXB formation via the He star SN mechanism and describe the method to incorporate their effect in a synthesis calculation in § 4. We discuss our assumptions for the parent population and the synthesis method in § 5. The results of the population synthesis calculations in comparison to observations as well as their dependence on the input parameters are discussed in § 6. Our conclusions are stated in § 7. Finally, the set of analytic approximations employed in our model is given in an Appendix.

2. DESCRIPTION OF THE EVOLUTIONARY CHANNEL

Low-mass X-ray binaries have donors of mass $\lesssim 1\ M_\odot$. As elaborated below, these donors were probably always of low mass. The primary of a LMXB progenitor, however, must be massive enough to produce a neutron star. Its helium core, exposed at the end of the common envelope phase, must therefore have been massive enough to reach core collapse. For these reasons, we need to consider a primordial binary system with an extreme mass ratio. The more massive star evolves much faster than its companion and is the first to fill its Roche lobe. The fact that initially the system had an extreme mass ratio affects its evolution in two ways: (1) The timescale for nuclear evolution of the primary is so much smaller than that of its companion that, when mass transfer begins, the secondary is practically still on the zero-age main sequence (ZAMS); and (2) as its mass increases, the secondary relaxes toward thermal equilibrium on its own thermal timescale, which is long compared to the mass transfer timescale, dictated by the thermal or dynamical timescale of the massive donor. Consequently, the transferred material cannot cool as it is accreted and the secondary swells up and fills its Roche lobe. In this way, a common envelope (CE) is created that engulfs the binary.

Even before the formation of the common envelope, when the massive primary approaches its Roche lobe radius, spiral-in of the secondary is initiated, as the primary's angular momentum at synchronism exceeds one-third of that of the orbit and the Darwin tidal instability sets in (Darwin 1879). With the formation of the common envelope, the secondary further spirals toward the core of the primary owing to frictional dissipation of the orbital energy. The details of the physical processes involved are not well understood, but it is generally accepted that, as energy is dissipated in the common envelope, the envelope expands and is eventually expelled. The orbital energy is assumed to be deposited in the envelope with an efficiency $\alpha_{\rm CE}$ (common envelope efficiency). If the orbital energy is sufficient, the binary system emerges with the secondary and the core of the primary orbiting each other. The post–common envelope orbit is considerably smaller than the initial one owing to the typically large ratio of the envelope mass to secondary mass (eq. [A8]).

Numerical calculations of the common envelope phase (for a review, see Iben & Livio 1993) show that its duration is orders of magnitude smaller than the nuclear timescales of both the donor and the accretor. Furthermore, Hjellming & Taam (1991) showed that the secondary remains practically unaffected at the end of the process, and the increase (or decrease) of its mass is insignificant ($\lesssim 1\%$). Accordingly, we may assume that at the end of the CE phase the secondary preserves its mass and is still on the ZAMS. In addition, model calculations show that, as a rule, mass transfer once started will continue until the donor star is stripped down to a composition boundary (Paczyński 1971). We may therefore assume that the mass of the post-CE primary is equal to the mass within its nuclear-burning core (or within the outermost nuclear-burning shell) at the moment it filled its Roche lobe. In this evolutionary scenario, the binary emerging from the common envelope evolves "quietly" as a detached system until the remnant core explodes as a supernova.

It should be noted that the binary evolution both before and after the CE phase is not conservative. The primaries of interest are so massive that wind mass loss is expected to take place before the primary fills its Roche lobe. This mass loss affects the structure and evolution of the primary as well as the orbital characteristics of the system. Moreover, the core of the primary emerging from the CE is still massive enough to suffer substantial wind mass loss in a way analogous to that of a Wolf-Rayet star. Once again the evolution of both the star and the orbit is affected.

The supernova explosion is a crucial event in the evolution of the LMXB progenitors. Most systems are disrupted, but some fraction of them must survive if they are to evolve further to become LMXBs. We will show later that both the survival fraction and the characteristic properties of the newly formed systems depend strongly on the existence and mean magnitude of a kick velocity imparted to the newborn neutron star.

The systems that survive the supernova event can come into contact via two physical processes: nuclear evolution of the secondary and shrinkage of the orbit (and hence of the Roche lobe) due to angular momentum losses. Depending on the nature of the secondary, the physical mechanism responsible for angular momentum losses may be gravita-

tional radiation and/or a magnetic stellar wind. Either way, the system comes into contact, and mass starts flowing from the secondary toward the neutron star. At the time of contact we call the system a zero-age low-mass X-ray binary (ZALMXB).

3. CONSTRAINTS AND LIMITS ON THE LMXB PROGENITORS

3.1. *Structural and Evolutionary Constraints*

Only a very small fraction of all binary systems follow the evolutionary channel described above. By demanding that a system survive all evolutionary stages in this specific sequence, we are able to constrain the characteristics and physical parameters of the initial binaries, the LMXB progenitors.

A number of constraints are imposed by this scenario (Webbink & Kalogera 1994):

1. *The primary must fill its Roche lobe before it explodes as a supernova.* The orbit of the progenitor cannot be arbitrarily large, since the system must reach interaction and enter common envelope evolution before the primary becomes a neutron star.

2. *The system must remain detached following the CE phase until the primary becomes a neutron star.* This is a twofold constraint: (1) The orbit at the end of the CE phase must be wide enough to accommodate the low-mass companion; (2) it must also be wide enough not to abort evolution of the remnant core prior to its supernova explosion. The post-CE primary is a helium star (He star) losing mass in a copious Wolf-Rayet (W-R) wind. Woosley, Langer, & Weaver (1995) have evolved mass-losing He stars with masses from 4 $M_\odot$ to 20 $M_\odot$ and found that they produce iron cores barely massive enough to collapse to a neutron star. We expect that an episode of mass transfer occurring early or midway in the evolution of the He star will arrest the growth of the iron core (by completely stripping away the helium envelope feeding it), thus preventing the formation of a neutron star.

3. *The system must remain bound after the supernova event.* Under the assumption of a symmetric supernova, there is an absolute limit on the amount of mass lost in the event for the binary to survive (Boersma 1961). If we take into account a kick velocity imparted to the newborn neutron star owing to an asymmetric core collapse, then survival depends on the magnitude and the direction of the kick.

4. *The mass transfer phase following the formation of the neutron star must be appreciably long lived.* In order for the system to become a LMXB with an appreciable lifetime, the companion to the neutron star must remain in equilibrium, and the mass transfer rate must not exceed the Eddington limit ($\dot{M}_{\rm Edd} \sim 10^{-8}\ M_\odot\ {\rm yr}^{-1}$). However, we will entertain the possibility that a system initially transferring mass at super-Eddington rates may find the mass transfer rate subsiding below that limit if the companion remains in thermal and hydrostatic equilibrium.

5. *The post-SN system must reach interaction in a Hubble time.* In order for a system to be included in the LMXB population, it must become a luminous X-ray source within a Hubble time. This means that the post-SN orbit must be small enough so that the secondary will fill its Roche lobe in $\sim 10^{10}$ yr, either due to its own evolution or due to the shrinkage of the orbit caused by angular momentum losses.

3.2. *Limits on the Parameter Space of LMXB Progenitors*

A binary system is characterized primarily by three parameters: the masses of the two stars, M_1 and M_2, and their orbital separation, A. Eccentricity is another characteristic, but we will neglect it here, assuming that tidal dissipation is efficient enough to destroy any initial eccentricity prior to actual mass transfer. For a scaleless distribution in orbital separation, as we will assume (§ 5.1), the distribution of separations of circularized orbits will be identical to that of the initial (eccentric) orbits, so long as the distribution of eccentricities does not itself vary significantly with separation over the range of interest. We can therefore assume equivalently that all the progenitors are formed with circular orbits. The constraints described qualitatively above substantially limit the range of values that M_1, M_2, and A can cover and yet produce LMXBs. In the calculation of these limits we use a number of approximate relations described in detail in the Appendix.

For specified masses[1] of the primary and its companion, the first of the constraints listed above sets an upper limit on the orbital separations of the progenitors. This limit corresponds to the primaries that first fill their Roche lobe just before core collapse. If we choose a value for $\alpha_{\rm CE}$, we can find the corresponding upper limit on the post-CE orbital separations.

The second of the constraints sets two lower limits on the orbital separations of the post-CE systems. One corresponds to the secondary just filling its Roche lobe at the end of the CE phase and the other to the He star primary filling its Roche lobe just prior to core collapse. During their evolution, He stars lose mass in a strong W-R wind and experience a rapid growth in radius, which is more severe as the stellar mass decreases (see Habets 1985; Woosley et al. 1995). The radii just prior to core collapse are considerably larger than those of the low-mass companions at ZAMS, so that the second of the constraints obviates the first one. The expansion of the secondary due to its own nuclear evolution prior to the supernova is invariably negligible, since the lifetime of the post-CE neutron star progenitor varies from 10^5 to 10^6 yr (depending on its composition at the end of the CE phase), which is orders of magnitude smaller than the evolutionary timescale of the low-mass companion.

The evolutionary sequences of mass-losing stars ($M < 40\ M_\odot$) presented by Schaller et al. (1992) show that massive stars suffer most of their mass loss only during the nuclear-burning phases of the core (H and He), when there is little or no radius expansion. In contrast, rapid growth in radius occurs between core hydrogen exhaustion and core helium ignition and again after helium exhaustion. During these phases of rapid expansion, the stellar mass is nearly constant (Fig. 1). If mass is lost to infinity from one or both components of a binary and carries with it a specific angular momentum equal to the orbital angular momentum per unit mass of its source component(s), then the binary separation varies as the inverse of the total mass of the binary (Jeans mode of mass loss). During core He burning, slow expansion but extensive mass loss characterizes massive stars, and we find that the rate of Roche lobe expansion due to systemic mass loss invariably exceeds the evolutionary rate of stellar expansion. Therefore, the primary can only fill its Roche lobe either (1) before central

[1] In this paper, radii and orbital separations are expressed in terms of $R_\odot$, masses in $M_\odot$, orbital periods in days, and time in years.

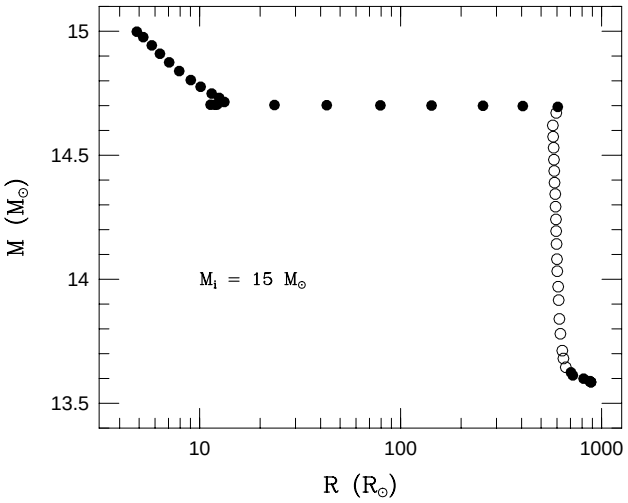

FIG. 1.—Mass as a function of radius for a mass-losing star of initial mass equal to 15 $M_\odot$. Open circles indicate the phase of core-helium burning (after Schaller et al. 1992).

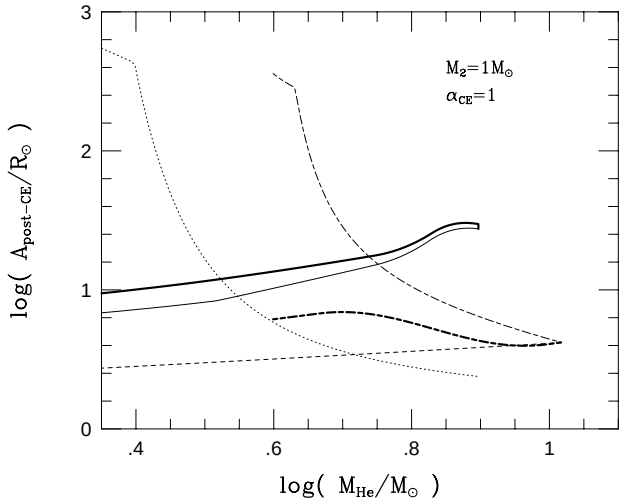

FIG. 2.—Limits on orbital separation and primary mass after the common envelope ejection for a 1 $M_\odot$ secondary and $\alpha_{CE} = 1$. Thick and thin lines correspond to upper and lower limits, respectively. *Thick solid line*: first Roche lobe overflow just prior to supernova; *solid line*: first Roche lobe overflow just after core-helium exhaustion; *dotted line*: He star with a C-O core (and *short-dashed line*: secondary) accommodated in the post-CE orbit; *thick long-short-dashed line*: first Roche lobe overflow just prior to core-helium ignition; *long short-dashed line*: He star with a helium core accommodated in the post-CE orbit. It is evident that a nonvanishing area of the parameter space is available to LMXB progenitors only if first Roche lobe overflow occurs after core-helium exhaustion.

He ignition or (2) after central He exhaustion. In the first case, the post-CE primary will be a helium star with a lifetime of $\sim 10^6$ yr (Habets 1985) losing mass in a Wolf-Rayet wind. These stars apparently lose most of their mass during this phase, which leads to some orbital expansion, but they also develop denser cores and much more extended envelopes at lower masses than would otherwise be the case. The net effect is to demand a much larger post-CE binary separation to accommodate the evolutionary expansion of the core He-burning primary than would be the case if it evolved at constant mass. In the second case, in which the common envelope is formed after central He exhaustion in the massive progenitor, the post-CE primary is again a helium star but has a C-O core. It is also more massive (by about 1.1 $M_\odot$) than the helium star in case (1) because of core growth during the hydrogen-shell burning phase experienced by the primary before CE formation. Furthermore, since helium has already been exhausted in the center, the helium star has also a shorter lifetime ($\sim 10^5$ yr) (Habets 1985) and therefore suffers minor further mass loss, which can be ignored (Woosley et al. 1995). Therefore, they remain massive enough that the growth in radius is mild, and hence the limit on the orbital separation is lower. The relation between the limits is depicted in Figure 2, from which it becomes evident that LMXB progenitors survive post-CE evolution up to the point of SN explosion *only* in the case that the common envelope is formed *after* central He exhaustion, at which point the initial primary has already lost a significant amount of its envelope due to its own wind.

In the event of a symmetric core collapse and a circular pre-SN orbit, the system will remain bound (constraint [3]) only if less than half of its initial total mass is lost in the explosion. The assumption of a circular orbit before the explosion is well justified, since the system has emerged out of a common envelope, a highly dissipative process. Given a symmetric collapse (in the frame of the primary), the binary will remain bound only if

$$(M_{\rm He} - M_{\rm NS}) < \frac{M_{\rm He} + M_2}{2} \quad \text{or} \quad M_{\rm He} < M_2 + 2M_{\rm NS}\,, \quad (1)$$

where $M_{\rm He}$, M_2, and $M_{\rm NS}$ are the (gravitational) masses of the neutron star progenitor, the secondary, and the neutron star, respectively.

The limits imposed on masses and radii of LMXB donors by the final two constraints listed above have already been studied in detail by Kalogera & Webbink (1996; hereafter Paper I). Here, we summarize their results:

In the case of conservative mass transfer, main-sequence donors less massive than $\sim 1.5\ M_\odot$ are stable against thermal timescale mass transfer, while those crossing the Hertzsprung gap are stable if their masses do not exceed $\sim 1.3\ M_\odot$. Donors that have evolved beyond the base of the giant branch are stable against mass transfer on a dynamical timescale and drive sub-Eddington mass transfer only if their masses are smaller than $\sim 1\ M_\odot$. However, the population of these donors is diminished by the constraint that their age must not exceed the galactic disk age, T. For $T = 10^{10}$ yr, the parameter space ($\log M_2$–$\log R_2$) occupied by donors first filling their Roche lobes beyond the base of the giant branch and transferring mass at sub-Eddington rates is extremely small (see Fig. 9*a* in Paper I) and vanishes altogether if angular momentum losses due to magnetic stellar winds are significant.[2] If super-Eddington mass transfer rates are allowed, but still with the constraint that donors remain in dynamical and thermal equilibrium, the limits on donor masses are extended to $\sim 2\ M_\odot$ on the main sequence and to $\sim 1.5\ M_\odot$ on the giant branch. However, it is not clear whether these systems will actually emerge as X-ray sources. Finally, there are two additional

[2] Magnetic stellar wind losses were inadvertently neglected in our estimates of initial mass transfer rates in Paper I. Only for giant branch donors is the division between sub- and super-Eddington systems measurably affected; none of the stability limits is affected.

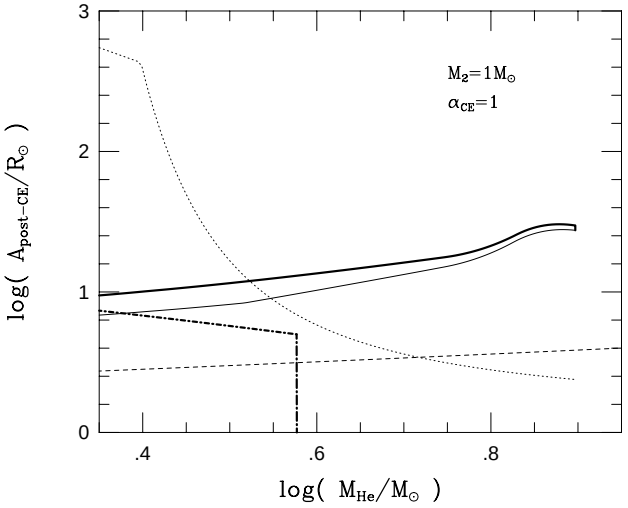

FIG. 3.—Limits on orbital separation and primary mass after the common envelope ejection for a 1 $M_\odot$ secondary and $\alpha_{CE} = 1$, in the case of a *symmetric* core collapse. Line-type coding is the same as in Fig. 2. In addition, *thick dot-short-dashed line*: mass transfer in the post-SN binary is initiated within 10^{10} yr; *thick dot-long-dashed line*: maximum He star mass for keeping the post-SN system bound. It is evident that no parameter space is available to LMXB progenitors.

groups of systems, with donors first filling their Roche lobes while on the main sequence or while crossing the Hertzsprung gap, that experience thermal timescale mass transfer but eventually recover equilibrium and enter a long-lived mass transfer phase. Those with donors filling their lobes in the Hertzsprung gap all subside to sub-Eddington rates and emerge as systems with giant branch donors. However, only a portion of those with the main-sequence donors will drive mass transfer at rates below the Eddington limit after recovering thermal equilibrium (see Fig. 6 in Paper I).

All relevant limits imposed on the post-CE orbital characteristics are illustrated in Figure 3 for $M_2 = 1.0\ M_\odot$ and $\alpha_{CE} = 1$ under the assumption of a symmetric supernova. Indeed, if we adhere to the requirement that mass transfer be sub-Eddington, we find no combination of limits that leaves viable sub-Eddington LMXB progenitors. We conclude that binaries could not form short-period LMXBs via this evolutionary channel if supernovae were symmetric, regardless of the rest of their characteristics, because the only systems that can survive mass loss in the supernova event are so wide (in order to accommodate the evolution of the core) that they will subsequently reach mass transfer only as the secondary ascends the giant branch. This process will take more than 10^{10} yr (if $M_2 \lesssim 1\ M_\odot$) or will result in super-Eddington mass transfer rates (if $1\ M_\odot \lesssim M_2 \lesssim 1.5\ M_\odot$) or will lead to dynamical instability (if $M_2 \gtrsim 1.5\ M_\odot$). The existence of short-period LMXBs therefore demands that one or more of the constraints be relaxed.

4. ASYMMETRIC SUPERNOVA EXPLOSIONS

Studies of the pulsar population (see, e.g., Harrison, Lyne, & Anderson 1993) show that it is characterized by a large scale height and high space velocities, providing observational evidence that, at their birth, pulsars are given a kick velocity, owing to an asymmetry associated with the supernova explosion. The magnitude of the kick is large enough to influence the kinematics of the pulsar population and certainly the orbital dynamics of a binary system hosting a neutron star progenitor. The constraints discussed in the previous section imply that, unless a kick velocity is imparted to the newborn compact star, it is essentially impossible to form short-period LMXBs via the evolutionary path considered here. Models attempting to explain the pulsar velocity distribution and the putative velocity–magnetic moment correlation (Dewey & Cordes 1987; Bailes 1989) require kick velocities with mean magnitudes of $\sim$100–200 km s^{-1}. However, a more recent study (Lyne & Lorimer 1994) of the pulsar population takes into account a selection effect against high-velocity pulsars and concludes that the mean pulsar velocity is $\sim$450 km s^{-1}. Additional evidence from supernova remnants and associated pulsar positions (Caraveo 1993; Frail, Goss, & Whiteoak 1994) supports the conclusion of high kick velocities. Although pulsar velocities do not directly reflect the birth velocities, these recent estimates do point toward high kick magnitudes. Any correlation between kick direction or magnitude and orbital axis or orbital velocity in a binary is at present purely conjectural, and hence we will assume that kick velocities are isotropically oriented in the center-of-mass frame of the collapsing component with a Maxwellian distribution in magnitude.

The interplay between the different limits discussed in the previous section changes dramatically if we relax the assumption of a symmetric supernova explosion. An asymmetric core collapse, imparting a kick velocity to the neutron star, breaks the one-to-one link between pre- and post-SN orbital parameters. Those constraints in Figure 3 that reflect post-SN conditions no longer sharply delimit possible LMXB progenitors. Systems that in the case of symmetric supernovae would have certainly been disrupted may now survive (if by chance the kick velocity has the right direction and magnitude), and, conversely, systems that would have survived may now be disrupted. Moreover, postsupernova orbits may now become smaller than the presupernova ones (which can never be the case in a symmetric core collapse), allowing the formation of short-period LMXBs. Thus, for the case of an asymmetric collapse, the limits imposed on the progenitors, after the ejection of the common envelope, are only the ones shown in Figure 4. In that case, a nonvanishing part of the parameter space may be populated by LMXB progenitors. The post-CE progenitors are Wolf-Rayet binaries, and for a 1 $M_\odot$ secondary they have primaries with masses $\sim$3.5–8 $M_\odot$, orbital separations $\sim$8–25 $R_\odot$, and orbital periods $\sim 1^d$–5^d. The corresponding limits on the primordial binaries are also shown in Figure 4; these O, B primaries have masses $\sim$13–25 $M_\odot$, orbital separations $\sim$800–1800 $R_\odot$, and orbital periods $\sim$1.5–5 yr.

The inclusion of a kick velocity imparted to the neutron star forces one to follow the evolution of an initial population of binaries and not of a single system. The stochastic element in this problem, of finding the distribution of binaries after an asymmetric supernova explosion, has been already addressed by Kalogera (1996). Assuming an isotropic Maxwellian distribution of kick velocities, she developed an analytical method of calculating the distribution of post-SN binary systems over eccentricity, orbital separations (before and after circularization), and systemic velocities. Here, we are interested only in the distribution of orbital separations of post-SN circularized orbits. Follow-

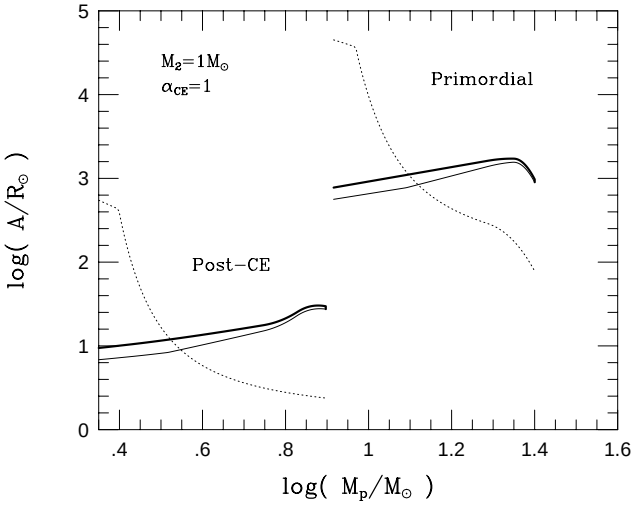

FIG. 4.—Limits on orbital separation and primary mass of primordial (O, B) and post–common envelope binaries with a 1 $M_\odot$ secondary, for $\alpha_{CE} = 1$. Line-type coding is the same as in Fig. 2.

ing the notation of Kalogera (1996), the distribution of systems over of the dimensionless separation $\alpha_c \equiv A_c/A_i$, where A_c and A_i are the circularized and pre-SN orbital separations, respectively, is given by

$$\mathscr{H}(\alpha_c) = \left(\frac{\beta}{2\xi^2}\right) \exp\left[\frac{-(\beta\alpha_c + 1)}{2\xi^2}\right] I_0\left(\frac{\sqrt{\beta\alpha_c}}{\xi^2}\right) \times \mathrm{erf}\left(z_o \sqrt{\frac{\beta}{2\xi^2}}\right), \quad (2)$$

where

$$\mathrm{erf}\,(x_0) \equiv \frac{2}{\sqrt{\pi}} \int_0^{x_0} e^{-x^2}\, dx\,,$$

$$z_0 = \sqrt{2 - \alpha_c - \frac{2c - \alpha_c}{c^2}}, \quad \frac{2c}{1+c} < \alpha_c < 2c$$

$$= \sqrt{2 - \alpha_c}, \quad 2c \le \alpha_c < 2$$

$$\beta = \frac{M_{NS} + M_2}{M_c + M_2}\,,$$

$$\xi = \frac{\sigma}{V_r}\,,$$

I_0 is the zeroth-order Bessel function, $\sigma = \langle V_k^2/3\rangle^{1/2}$, V_r is the relative orbital velocity of the two stars in the pre-SN binary, and c is the ratio of the radius of the secondary to the pre-SN orbital separation.

Convolving the above distribution with that of the pre-SN binaries over masses and orbital separations, as defined by the limits already discussed, enables us to map precisely the distribution of post-SN binaries and synthesize the population of nascent LMXBs.

5. POPULATION SYNTHESIS

5.1. *Parent Binary Evolution*

Having described the criteria that select LMXB progenitors from a parent binary population, we require a statistical description of this primordial population to produce quantitative results. We therefore assume that the primordial binaries can be characterized by three parameters : the mass of the primary M_1, the mass ratio $q \equiv M_2/M_1$ (M_2 being the mass of the secondary star), and the orbital separation of the system A. In selecting an initial distribution of binaries over these parameters, we are guided by the results of a detailed analysis by Hogeveen (1991), but with some important differences at small mass ratios, where observational constraints are virtually nonexistent.

We have adopted the field star initial mass function (IMF) derived by Scalo (1986) as a good representation of the primary mass distribution. Based on his results, we are able to fit the IMF of stars more massive than 0.3 $M_\odot$ with a single power law of the form

$$\Xi(M) = \Xi_0\, M^{-2.7} \text{ stars pc}^{-2} \text{ yr}^{-1}\, M_\odot^{-1}\,,$$
$$\Xi_0 \simeq 6.83 \times 10^{-10}\,. \quad (3)$$

If we assume that the galactic disk has an exponential surface density with a scale length of 4 kpc and that the distance of the Sun from the galactic center is 8 kpc, then we estimate the effective radius of the galactic disk to be 15 kpc. The birthrate of primaries per unit logarithm of mass, integrated over the entire galactic disk, is then

$$f_1(\log M_1) \simeq 1.112 M_1^{-1.7} \text{ yr}^{-1} (\log M_\odot)^{-1}\,. \quad (4)$$

The distribution of orbital separations is assumed to be inversely proportional to A (Abt 1983), normalized to a wide range of initial separations up to 10^6 $R_\odot$. This assumption may appear inconsistent with more recent results regarding the orbital period distribution of solar-type binaries (Duquennoy & Mayor 1991). However, we note that the range of orbital separations, hence orbital periods, of interest to us is extremely narrow, from $\sim$2 yr to $\sim$5 yr, so that our results are not sensitive to the specific shape of the broader distribution. Furthermore, our choice of the functional form and normalization is consistent with the one used by Hogeveen (1991) in his study of the mass ratio distribution, the results of which we have chosen to adopt.

The mass ratio distribution of unevolved binaries of interest to us is quite uncertain. It is empirically known only in the limit of approximately equal component masses and for relatively close binaries. Results obtained by Hogeveen (1991) show that for $q \gtrsim 0.35$, the mass ratio distribution at long orbital periods is described by an IMF-like power law ($\propto q^{-2.7}$). However, we need to extrapolate to very small values of q (<0.1). For this range of values, it is often assumed that the distribution flattens, but this is in truth an ad hoc assumption because the contribution of such extreme mass ratio systems to the observed distribution of spectroscopic or eclipsing binaries at long periods (>1 yr) is negligible. Instead we have chosen to adopt an IMF-like q-distribution, even for very small values of q. By making this assumption and demanding that the normalization accords with observation as $q \to 1$, we must explicitly allow for the possibility that our primordial systems are not only binary but multiple. In doing so, we recognize that the presence of additional stellar components modifies our pool of progenitor binaries in two ways : (1) an inner binary may abort evolution of the primary by mass exchange, thwarting its expansion to a common envelope stage involving the secondary component of interest to our scenario; and (2)

triple systems are dynamically stable only if the period ratio between outer and inner orbits exceeds some critical value. Regarding the first of these two elements, an inner binary with a secondary component *less* massive than the outer one of interest to us is very unlikely to be of any consequence: the inner binary will succumb to common envelope evolution, but it is incapable of extracting enough energy to eject the envelope before merging—the outer binaries of interest to us typically only barely manage to survive. We therefore exclude from our progenitor pool only those multiples in which the inner binary contains a more massive secondary than the outer. Similarly, in regard to the second element, dynamical instability of a triple star typically leads to ejection of the least massive component (Harrington 1975). We therefore exclude from our progenitor pool only those multiples in which a third component, more massive than the secondary of interest to us, lies within a critical period (or separation) ratio of the secondary orbit. Following Kiseleva, Eggleton, & Anosova (1994), we adopt a critical period ratio of 6.3 (separation ratio $\simeq 3.4$) for the extreme mass ratios of interest here. All systems containing third components more massive than our secondary are therefore excluded, from a maximum orbital period of 6.3 times that of interest down to a minimum physically allowable separation, which we take (for simplicity) to be twice the primary radius. Assuming that binary and multiple stars are chosen from a parent population according to Poisson statistics (i.e., that they are independent, uncorrelated events), we modify our simple inverse distribution in A and power-law distribution in q by a factor representing the Poisson probability that neither of the above strictures is violated:

$$g(q, A) = \frac{0.075}{A}\, 0.04 q^{-2.7} \times \exp\left(- \int_{2R(M_1)}^{A \cdot 6.3^{2/3}} \int_{q}^{1} 0.075 A'^{-1} 0.04 q'^{-2.7}\, dA'\, dq' \right). \quad (5)$$

A plot of this assumed distribution over mass ratio, q, for specified primary mass, M_1, and orbital separation, A, is shown in Figure 5. It bears reemphasizing that this distribution is unverifiable by current observation for $q \lesssim 0.35$. The adoption of equation (5) is motivated by three factors : (1) it is consistent with observed rates of duplicity and mass ratio, where these are detectable, for binary separations of interest to us; (2) it is a logical extrapolation of that observable part of the distribution to the extreme mass ratios of interest to us, without the invocation of ad hoc breaks or cutoffs; and (3) it provides a consistent formalism for future modeling of LMXB formation by triple star evolution.

We can transform equation (5) to a distribution over $\log M_2$ and $\log A$, $h_{\rm in}(\log M_2, \log A)$, using the definition of q. The distribution representing the primordial binary population then becomes

$$F_{\rm in}(\log M_1, \log M_2, \log A) = f_1(\log M_1) \times h_{\rm in}(\log M_2, \log A)\,. \quad (6)$$

The range of values covered by the three parameters is dictated by the evolutionary selection criteria already discussed.

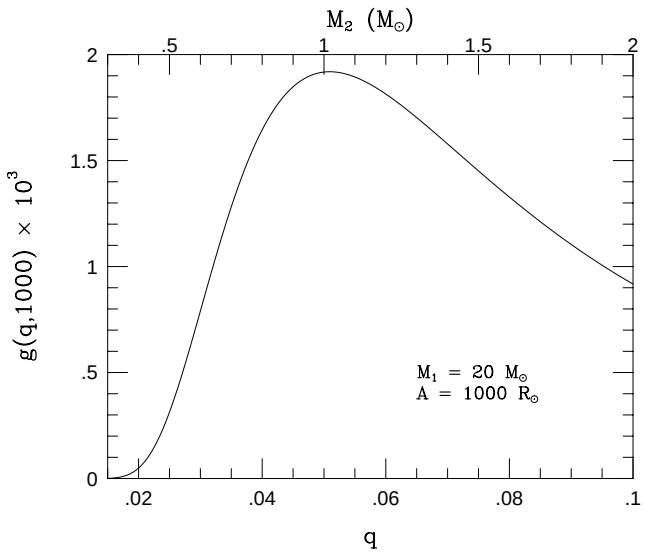

FIG. 5.—Distribution of primordial binaries with primary mass $M_1 = 20\ M_\odot$ and orbital separation $A = 1000\ R_\odot$ over mass ratio, q. The corresponding secondary masses, M_2, are also shown.

5.2. *Method*

Having defined the parent binary population, we are able to follow its transformation as the systems evolve through the various evolutionary stages. This is done by identifying the system parameters at the end of each stage and their dependence on the corresponding parameters at the beginning of each phase and by transforming the distribution function according to these dependences. These transformations are performed analytically, so that at each stage prior to the explosion, the distribution function of binaries can be expressed explicitly. At the supernova stage, the pre-SN function is convolved with the distribution over post-SN circularized separations (eq. [2]), and the product is integrated numerically now over pre-SN helium star masses and orbital separations. This method offers major advantages over Monte Carlo techniques as it is free of any statistical errors and in principle allows us to have an infinite resolution in the final LMXB parameters. This high resolution reveals even the most subtle features in the nascent LMXB distribution and permits us to trace back the origin of these features. In what follows, we briefly describe the procedure for each evolutionary stage of interest.

From all the systems represented by $F_{\rm in}$, we are interested only in those that experience a common envelope phase. The post-CE systems are characterized by the secondary mass M_2 (assumed unchanged by CE evolution), the orbital separation $A_{\rm post\text{-}CE}$, and the mass of the remnant core $M_{\rm He}$, which depends only on the primary mass. Using the relations connecting the pre- and post-CE binary parameters we can find analytically the transformed post-CE distribution function:

$$F_{\rm CE}(\log M_{\rm He}, \log M_2, \log A_{\rm post\text{-}CE}) = F_{\rm in} \times J\left(\frac{\log M_1, \log M_2, \log A}{\log M_{\rm He}, \log M_2, \log A_{\rm post\text{-}CE}} \right). \quad (7)$$

Since $\partial \log A / \partial \log A_{\rm post\text{-}CE} = 1$ (eq. [A8]), M_2 is unchanged, and $M_{\rm He}$ is a function only of M_1 (eq. [A3]), the distribution of post-CE orbital separations and secondary masses for a

specific choice of $M_{\rm He}$ is simply a homologous transformation of their pre-CE distribution at the corresponding value of M_1.

The post-CE primary, $M_{\rm He}$, has already exhausted helium in its core, since the initial primary entered common envelope evolution after core-He exhaustion. The timescale for nuclear evolution of the C-O core until collapse is $\sim 10^5$ yr (Habets 1985) and is so short that the helium star is essentially unaffected by wind mass loss (Woosley et al. 1995). Therefore, the pre-SN distribution of binaries is identical with the one just after the CE phase. The secondary is still on the main sequence when the supernova occurs.

By convolving the pre-SN distribution with the survival probability distribution for the supernova explosion, $\mathscr{H}(\alpha_c)$ (eq. [2]), we can obtain the distribution function, $Z(\log M_2, \log A_{\rm post\text{-}SN})$, of post-SN circularized orbital separations $A_{\rm post\text{-}SN}$ and secondary masses M_2 by integrating over $M_{\rm He}$ and $A_{\rm pre\text{-}SN}$. In performing this transformation, we assume that all He stars leave a remnant neutron star of the same gravitational mass (see also Woosley et al. 1995) of 1.4 $M_\odot$. The post-SN distribution thus becomes a two-variable function of M_2 and $A_{\rm post\text{-}SN}$:

$$Z(\log M_2, \log A_{\rm post\text{-}SN}) = \int_{\log M_{\rm He}{}^{\rm min}}^{\log M_{\rm He}{}^{\rm max}} \int_{\log A_{\rm pre\text{-}SN}{}^{\rm min}}^{\log A_{\rm pre\text{-}SN}{}^{\rm max}} \zeta \times (d \log A_{\rm pre\text{-}SN}) d(\log M_{\rm He}) , \quad (8)$$

where

$$\zeta \equiv F_{\rm CE} \times \mathscr{H}(\alpha_c) \times \alpha_c \ln 10 ,$$

and $\alpha_c \ln 10$ is the Jacobian corresponding to the variable transformation from $\alpha_c = A_{\rm post\text{-}SN}/A_{\rm pre\text{-}SN}$ to $\log A_{\rm post\text{-}SN}$. The limits of the integration over $\log A_{\rm pre\text{-}SN}$ depend on both $M_{\rm He}$ and M_2; those for the integration over $M_{\rm He}$ depend on M_2, according to the constraints discussed in § 3.

We have assumed here that both synchronization and circularization of the binary occurs relatively soon and certainly prior to the time the secondary overflows its Roche lobe. The assumption is well justified since the timescales for both processes for detached systems are significantly shorter than the evolutionary timescale of the secondary as well as the timescale for angular momentum losses due to magnetic braking. As the binary approaches Roche lobe overflow, the timescales rapidly decrease down to tens to thousands of years (e.g., for $R_L/R_2 \simeq 2$; see Zahn 1977, 1989).

Systems surviving the supernova event do not all form LMXBs. Binaries must still evolve further toward Roche lobe overflow of the secondary for mass transfer to be initiated. At this stage binary evolution is driven by nuclear evolution of the secondary and loss of angular momentum, and hence shrinkage of the Roche lobe around the secondary. We consider two mechanisms responsible for the loss of angular momentum: gravitational radiation (eq. [A11]) and magnetic braking (eq. [A13]). In the latter process, a wind from the secondary, locked onto the stellar magnetic field, drives angular momentum away from the star. Assuming that the companion is maintained in synchronization with the orbit by tidal dissipation, it follows that the binary loses angular momentum (Verbunt & Zwaan 1981). This angular momentum loss affects the orbital characteristics considerably, whereas the mass-loss rate is assumed negligible. For very low mass secondaries ($M_2 \leq 0.37\ M_\odot$) that are fully convective, we assume that magnetic braking is negligible, in accordance with arguments advanced to explain the 2–3 hr gap in the orbital period distribution of cataclysmic variables (Rappaport, Verbunt, & Joss 1983). For these masses, angular momentum loss due to gravitational radiation alone is considered.

It should be noted that studies of the magnetic braking mechanism rely upon measurements of rotational velocities of solar-type stars (Verbunt & Zwaan 1981). More massive stars develop radiative envelopes that are expected to diminish the dynamo generation of magnetic fields and hence the effect of magnetic braking. In accordance with this, massive stars appear to rotate much faster than low-mass stars. We have adopted the functional form used by Rappaport et al. (1983) (with their index $\gamma = 2$), but modifying the braking efficiency for stars more massive than the Sun by introducing a cutoff factor, b, dependent only on stellar mass. Using observed mean rotational velocities for main-sequence stars, we were able to estimate the efficiency factor, $b(M_2)$:

$$\begin{aligned} b(M_2) &= 0 , & M_2 &\leq 0.37\ M_\odot , \\ &= 1 , & 0.37\ M_\odot &< M_2 \leq 1.03\ M_\odot , \\ &= \exp\,[-4.15(M_2 - 1.03)] , & M_2 &> 1.03\ M_\odot . \end{aligned} \quad (9)$$

This expression for the magnetic braking efficiency reproduces the rotation velocities of main-sequence stars of spectral types F5 and F0 (Allen 1973) assuming that they are born at rotational breakup and neglecting evolutionary changes in mass and radius. Main-sequence stars of earlier spectral type show no evidence of magnetic braking. Using more recent data (see, e.g., Fukuda 1982; Kawaler 1987) leads to somewhat different expressions for $b(M_2)$ but has no qualitative effect on our results. Because of the assumption of initial maximum rotation, the above estimate is actually an *upper* limit to the magnetic braking efficiency factor.

The last step in evolving the distribution function Z is to transform the post-SN systems to nascent LMXBs. We set the radius of the secondary (eq. [A9] in Paper I) equal to its Roche lobe radius (eq. [A7]) and eliminate the time by using either equation (A12) or equation (A14). The resulting equation can be solved numerically for the orbital separation, A_X, at the onset of the mass transfer phase. In this way we are able to find the distribution over orbital separation, A_X, and donor mass, M_2, of the LMXB progenitors:

$$\Phi_A(\log M_2, \log A_X) = Z \times \left| \frac{\partial \log A_{\rm post\text{-}SN}}{\partial \log A_X} \right| . \quad (10)$$

The derivative in the above equation is calculated analytically. With one last transformation we obtain the distribution over donor mass and orbital period, $\Phi_P(\log M_2, \log P_X)$.

6. RESULTS

6.1. *A Reference Model*

Results from our population synthesis calculations are illustrated in Figures 6*a* and 6*b* for a prototypical choice of input parameters, which we shall deem our reference case. The two frames of this figure show zero-age LMXB distributions, $\Phi(\log M_2, \log P_X)$, for systems initiating sub-Eddington mass transfer only (Fig. 6*a*) and for both sub-Eddington and super-Eddington systems (Fig. 6*b*). The constraints delineating these regions were discussed in

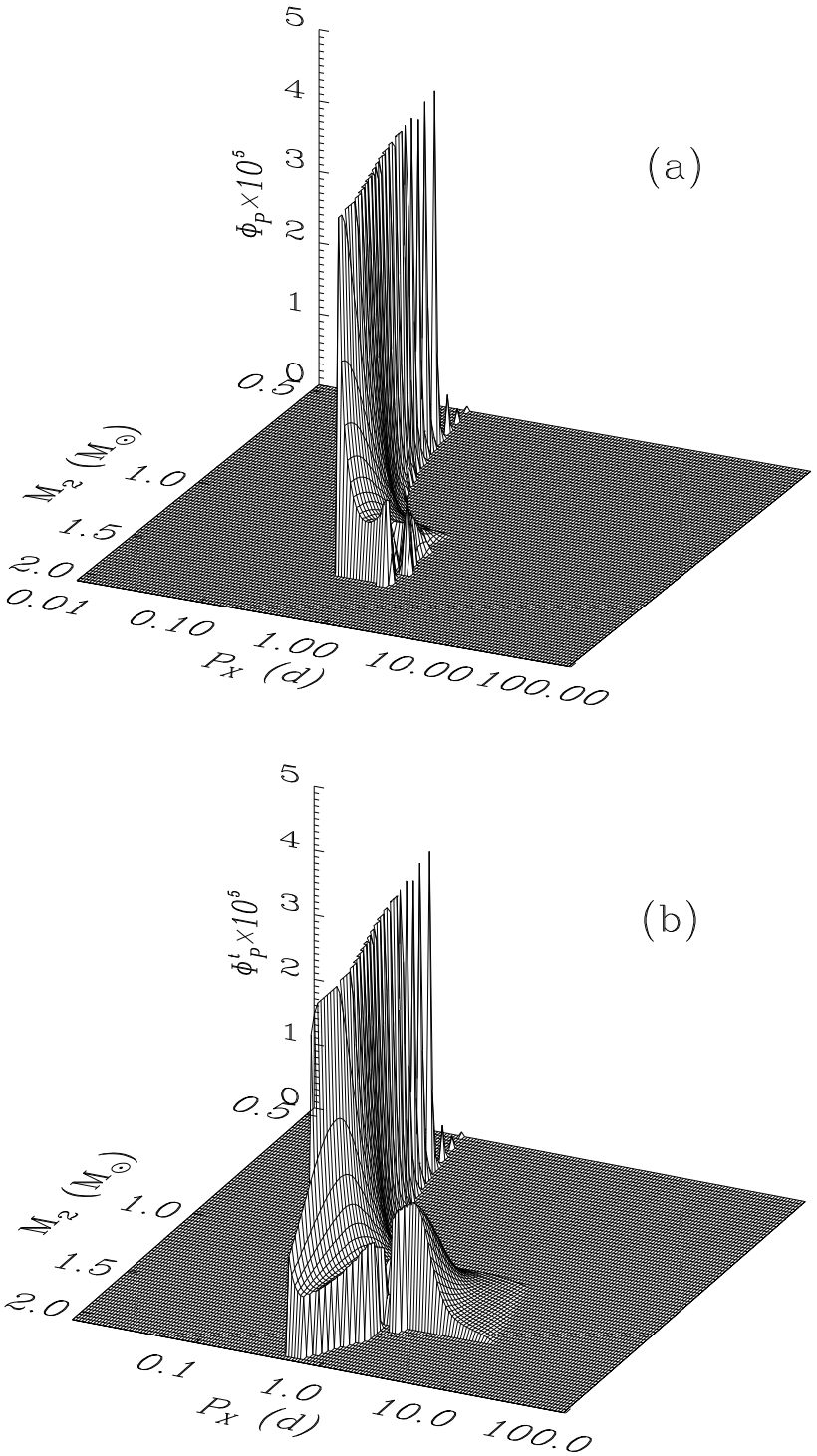

FIG. 6.—Distribution of nascent LMXBs, $\Phi_P(\log M_2, \log P_X)$, over donor mass, M_2, and orbital period, P_X, for $\langle V_k^2 \rangle^{1/2} = 300$ km s^{-1} and $\alpha_{CE} = 0.3$. Mass transfer at (*a*) sub-Eddington rates and (*b*) both sub- and super-Eddington rates.

Paper I and are illustrated again here in Figure 7, where the regions are labeled S_E and S^E, respectively. Our choices of values for free parameters in this reference case have been made in such a way as (1) to define a plausible extreme or (1) to characterize the model distribution at the threshold value of a specific parameter, that is, at a value where its influence on the resulting models changes character. Thus, for example, our choice of mass ratio distribution (eq. [5]) defines a plausible upper limit to the frequency of the massive binaries with extreme mass ratios that feed our evolutionary channel, since the Poisson cutoff invoked in equation (5) (an upper limit to the number of close companions a massive star may accommodate within the limits of dynamical stability) is taking effect in just the range of companion masses of interest (see Fig. 5). For the common envelope ejection efficiency, we choose $\alpha_{CE} = 0.3$, because below this value the survival window (the region bounded by thick and thin solid lines in Fig. 3) disappears rapidly below the lower limits to postsupernova binary separation imposed by the need to accommodate both the helium star

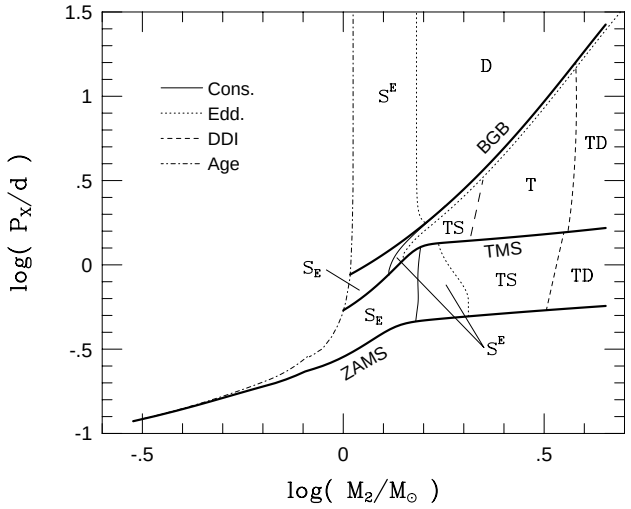

FIG. 7.—Limits on donor masses, M_2, and orbital periods, P_X, of binaries at the onset of mass transfer for a population of age 10^{10} yr. Heavy solid lines mark the loci of zero-age main sequence stars (ZAMS), terminal main-sequence stars (TMS), and stars at the base of the giant branch (BGB). *Dot-dashed line*: maximum orbital periods for mass transfer in a Galactic disk population of age 10^{10} yr; *thin solid lines*: maximum donor masses for thermal stability on the main sequence and in the Hertzsprung gap, assuming conservative mass transfer; *dotted lines*: maximum donor masses for thermal stability on the main sequence and in the Hertzsprung gap, and for dynamical stability on the giant branch, all in the limit that all mass lost from the donor is also lost from the binary; *short-dashed lines*: minimum donor masses for the development of a delayed dynamical instability; *long-dashed lines*: maximum donor masses for regaining thermal equilibrium after an initial mass transfer phase on a thermal timescale.

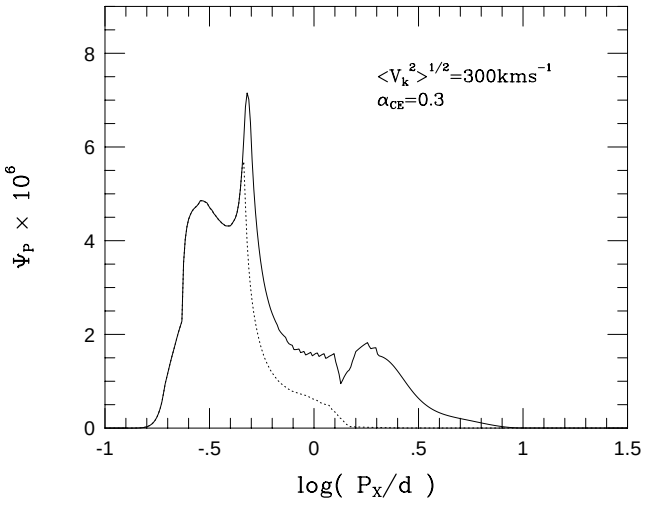

FIG. 8.—Distribution of nascent LMXBs, $\Psi_P(\log P_X)$, over orbital period, P_X, for $\langle V_k^2 \rangle^{1/2} = 300$ km s^{-1} and $\alpha_{CE} = 0.3$. *Solid line*: both sub- and super-Eddington systems, and *dotted line*: only sub-Eddington systems.

core of the primary (the dotted line in Fig. 3) and its companion (the thin dashed line in Fig. 3). Our choice of rms kick velocity for the reference case, $\langle V_k^2 \rangle^{1/2} = 300$ km s^{-1}, equates approximately to the maximum pre-SN relative orbital velocities and therefore lies very near the peak in their survival probability in the zero-age LMXB population.

Within the age and stability limits set by Figure 7, the general features seen in Figures 6*a* and 6*b* are the result primarily of a competition between nuclear evolution of the donor stars and angular momentum loss from the binary. The prominent ridge extending toward low companion masses and low orbital periods is due to systems with essentially zero-age donors, brought to Roche lobe contact owing to loss of angular momentum. This ridge along the ZAMS disappears for donors more massive than $\sim 1.4\ M_\odot$ because at these masses angular momentum losses due to magnetic braking become inefficient (eq. [9]). For donors more massive than $\sim 1\ M_\odot$, nuclear evolution becomes increasingly important, and not all post-SN systems experience orbital shrinkage. As a result, a minimum appears in the distribution at orbital periods of about 1 day. Systems with donors on the giant branch appear only in the super-Eddington population. They form the broad peak at long periods between donor masses $\sim 1\ M_\odot$ and $\sim 1.5\ M_\odot$ and have reached contact because of the advanced nuclear evolution of the donor.

The competition between angular momentum losses and nuclear evolution is also evident in the distribution over orbital periods, $\Psi_P(\log P_X)$, obtained by integrating Φ_P over $\log M_2$, and plotted in Figure 8. The first peak at $\sim 0^d.3$ arises from the peak in the mass ratio distribution (see Fig. 5), whereas the peak at $\sim 0^d.5$ is the result of the flattening of the ZAMS radius-mass relation above $\sim 1.3\ M_\odot$, which compresses a relatively wide range of donor masses into a narrow range of periods. The valley at $\sim 1^d$ is a result of magnetic braking evacuating this range. Systems with evolved donors that transfer mass at super-Eddington rates populate the "bump" at longer periods. These systems may not at first appear as luminous X-ray sources, as we anticipate that their dense super-Eddington outflows will quench X-ray emission. Nevertheless, as the donor mass decreases, mass transfer may subside to sub-Eddington rates, and the systems will then appear as LMXBs with donors on the giant branch.

We note in passing that Figure 8 also bears witness to the power of the analytical technique used for these synthesis calculations to reveal features that are very difficult and computationally expensive to identify in Monte Carlo approaches. A case in point is the inflection point visible at $\sim 0^d.23$, below the shortest period maximum. This feature is in fact an artifact of the ZAMS radius-mass relation we have adopted in this work (eq. [A1] in Paper I), which is discontinuous in its first derivative at $M_2 \simeq 0.8\ M_\odot$. With an analytic approach, we have the power in principle to increase resolution within a limited range of parameter space, as desired, without being obliged to do so everywhere and without suffering the Poisson noise inherent in Monte Carlo calculations.

6.2. *Observable Properties of the LMXB Population*

Despite three decades' effort in X-ray astronomy, our knowledge of the underlying structural properties of LMXBs is still extremely limited and fragmentary. Orbital periods, for example, are known only for a small minority of systems, a large fraction of LMXBs lack optical counterparts (because of low intrinsic optical luminosity and heavy interstellar extinction), and dynamical mass estimates from spectroscopic orbits are nearly absent outside that collection of soft X-ray transients that evidently contain black hole accretors of mass $> 3\ M_\odot$ (and that cannot originate through the formation channel modeled here). Nevertheless,

TABLE 1

CHARACTERISTICS OF THE LMXB POPULATION

PARAMETER	REFERENCE MODEL[a]		OBSERVED
	Sub-Eddington	Super-Eddington	
Birthrate (yr^{-1})	2×10^{-6}	1.2×10^{-6}	2×10^{-7}
Total X-ray luminosity (ergs s^{-1})	2.7×10^{40}	...	2×10^{39}
Fraction of systems with $P_X < 20\ h$	0.94	0.35	0.75–0.94
Fraction of NS accretors	0.91	...	$\gtrsim 0.4$
Center-of-mass velocity dispersion (km s^{-1})	150	127	183

[a] Input parameters: common envelope efficiency $\alpha_{CE} = 0.3$, rms kick magnitude $\langle V_k^2 \rangle^{1/2} = 300$ km s^{-1}, mass-ratio power-law index $x = 2.7$, and maximum baryonic neutron star mass $M_{NS}^{max} = 2.64\ M_\odot$.

there are several bases, summarized here in Table 1, on which a comparison may be made between global observational properties and the results of population synthesis models. The origin of the observational estimates contained in Table 1 is described below; theoretical estimates are listed separately for those systems that transfer mass initially at sub-Eddington rates (regions S_E, which we expect to remain LMXBs throughout this phase of interaction) and those initially super-Eddington (regions S^E, which we expect to contribute to the observed LMXB population only later during interaction, if at all). It must be emphasized here that the values of free parameters defining our reference model, from which results are extracted in Table 1, were chosen to aid in characterizing the dependence of model results on those parameters; they have not been chosen to optimize agreement between model and observation. The reader may glean some sense of the adjustments required from the discussion of parameter dependences which will follow below.

Some explanations are warranted for the entries in Table 1.

Birthrate.—We estimate the birthrate of the observed population from the catalogs of galactic LMXBs by van Paradijs (1995) and Bradt & McClintock (1993). Black hole candidates and LMXBs in globular clusters have been excluded. Distance estimates and mean X-ray luminosities of individual systems were drawn, where available, from those catalogs. The birthrate in steady state then follows from summing the observed mean X-ray luminosities and dividing by an average initial donor star mass (assumed to be 1.2 $M_\odot$, as suggested by the synthesis results), and assuming an X-ray production rate of 1.86×10^{20} ergs g^{-1} of accreted matter. The theoretical birthrates quoted here exclude any contribution from possible LMXB progenitors that may emerge from thermal timescale mass transfer, regions MS_2 and HG_2 in Figure 5 of Paper I; the birthrates for their immediate progenitors are, respectively, 2×10^{-6} yr^{-1} for region MS_1 and 1×10^{-6} yr^{-1} for region MS_2, in our reference model.

Total X-ray luminosity.—For comparison, we also include in Table 1 estimates of the observed and theoretical total X-ray luminosity for Galactic disk LMXBs. We derive a statistical (Poisson) uncertainty in the observed luminosity of $\pm 30\%$ but expect the true uncertainty to be substantially greater due to systematic errors (from spectral fittings and distance estimate errors). Since the deduced estimate of the birthrate of observed LMXBs follows directly from their total X-ray luminosity, this entry does not in reality provide a new benchmark for comparison, but it does strip away some of the assumptions applied above to deduce an observed birthrate. We apply the same assumptions instead to the synthesis models to convert birthrates to total X-ray luminosity but now employ the actual donor mass distribution produced by those models, instead of an average value.

Fraction of short-period systems.—Secular evolution among LMXBs produces a natural bifurcation in their evolution, with short-period systems ($P_X \lesssim 20$hr) driven to shorter orbital periods by angular momentum loss, and long-period systems driven to longer periods by nuclear evolution of the donor star (Taam, Flannery, & Faulkner 1980; Pylyser & Savonije 1989). This behavior provides a basis for comparison between theory and observation, even though our synthesis models do not address secular evolution in the LMXB state. Unfortunately, orbital periods are known for only 30% of galactic LMXBs; of the 24 systems with known periods, 18 fall into the short-period group. The observational upper limit quoted in Table 1 reflects our expectation that the higher optical/infrared luminosities of donors in longer period systems favor detection of their orbital periods, so that LMXBs with undetected periods are more likely to belong to the short-period group. It is important to note as well that the theoretical estimates listed for our reference case are probably lower limits, in that they reflect relative birthrates of short- and long-period systems, and do not account for the shorter lifetimes expected among longer orbital period systems.

Fraction of neutron star accretors.—A significant fraction of the neutron stars in our model populations (at least among those transferring mass at sub-Eddington rates) may be driven to gravitational collapse during their X-ray lifetime and become stellar black holes. An observational lower limit to the fraction of LMXBs containing neutron stars, quoted in Table 1 is set by those showing X-ray pulsations or classical X-ray bursts (see van Paradijs 1995). To obtain a theoretical estimate for this fraction, we adopt the equation of state (AV14/UVII) developed by Wiringa, Fiks, & Fabrocini (1988), which represents the most complete microscopic calculations available at present; this equation of state predicts maximum gravitational and baryonic (nonrotating) neutron star masses of 2.13 $M_\odot$ and 2.64 $M_\odot$, respectively (Cook, Shapiro, & Teukolsky 1994). Model systems with total baryonic mass exceeding 2.64 $M_\odot$ are considered to contain black hole accretors only once the accretor mass passes that threshold.

We must emphasize that black hole formation through accretion-induced neutron star collapse is incapable of explaining the existence of the low-mass black hole soft X-ray transients A0620−00 (V616 Mon), GS 2023+338 (V404 Cyg), GS 1124−684 (GU Mus), GRO J1655−40, GS

2000+25 (QZ Vul), and H1705−250 (V2107 Oph) (Cowley 1994; Bailyn et al. 1995; Charles & Casares 1995; Remillard et al. 1996). In each of these systems, lower limits to the masses of their compact components, derived dynamically from the reflex orbital motion of their donor stars, clearly exceed the maximum total mass of any of our modeled systems: $1.4\ M_\odot + 1.5\ M_\odot = 2.9\ M_\odot$. At least one other evolutionary channel is required (Eggleton & Verbunt 1986; Romani 1992).

Systemic velocities.—We have derived an observed velocity dispersion from the tabulation by Johnston (1992) of heliocentric radial velocities of 15 LMXBs, correcting for solar motion and for differential galactic rotation, using her distance estimates and the galactic rotation model of Clemens (1985), and assuming isotropic peculiar velocities with respect to uniform rotation on cylinders. Neither the rotation model nor the assumption of isotropic peculiar velocities can be strictly valid, but the observed velocity dispersion is more seriously suspect because of distance errors, since differential rotation corrections are large, and because of small-number statistics. The theoretical velocity dispersions in Table 1 reflect one-dimensional peculiar velocities at birth; virialization within the galactic potential should reduce them by a factor of $2^{1/2}$, since the hiatus between supernova explosion and the onset of mass transfer as an LMXB significantly exceeds a galactic dynamical timescale for the overwhelming majority of model systems.

6.3. *Parameter Studies*

Although one should treat the observed quantities listed in Table 1 with some caution, for reasons outlined above, it is instructive to explore how the theoretical quantities listed there respond to variations in the principal input parameters to our population models: (1) the efficiency of common envelope ejection, α_{CE}; (2) the rms kick velocity imparted to a newborn neutron star, $\langle V_k^2 \rangle^{1/2}$; (3) the initial mass ratio distribution; and (4) the maximum neutron star mass. These dependencies are summarized semi-quantitatively in Table 2 and discussed physically below.

Common envelope efficiency.—As illustrated in Figure 3, progenitor systems of given donor star mass populate only a narrow range of post–common envelope orbital separations. That range shifts to smaller separations for smaller companion masses (less orbital energy available for envelope ejection) or for small ejections efficiencies, α_{CE} (less efficient use of available orbital energy). Since the lower limits to binary separations are fixed by Roche lobe constraints, reductions in α_{CE} therefore result in (1) progressive loss of the lowest mass companions from the pool of donor stars, and (2) progressive loss of the longest period component of the survivor pool. The loss of low-mass donors suppresses the short-period extreme of the LMXB orbital period distribution. For $\alpha_{CE} \lesssim 0.3$, the peak of the donor mass distribution no longer survives, and the birthrate falls precipitously (Fig. 9). Since asymmetric supernovae cannot produce circularized postsupernova separations exceeding

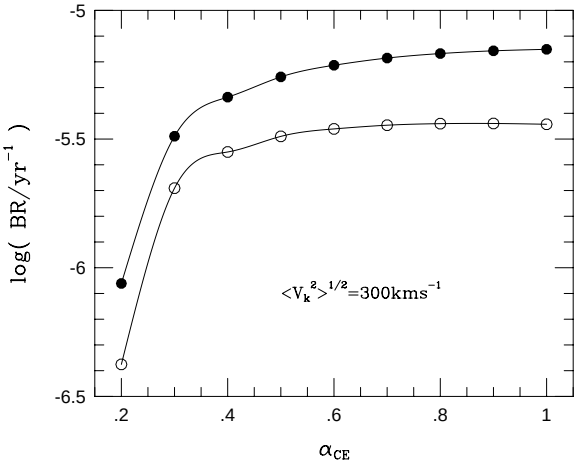

FIG. 9.—Total birthrate of sub-Eddington only (*open circles*) and sub- and super-Eddington combined (*filled circles*) nascent LMXBs as a function of common envelope efficiency α_{CE} for $\langle V_k^2 \rangle^{1/2} = 300$ km s^{-1}.

TABLE 2

EFFECTS OF INPUT PARAMETERS

Reference Model	α_{CE} (0.3)	$\langle V_k^2 \rangle^{1/2}$ (300 km s^{-1})	x (2.7)	M_{NS}^{max} (2.64 $M_\odot$)
Birthrate[a] and total X-ray luminosity[b]	Declines slowly as α_{CE} decreases from 1.0 to 0.3, but plummets rapidly for $\alpha_{CE} \lesssim 0.3$	Declines slowly for $\langle V_k^2 \rangle^{1/2} \gtrsim 200$ km s^{-1}; S_E (and S^E for $\alpha_{CE} \lesssim 0.6$) populations drop rapidly as $\langle V_k^2 \rangle^{1/2} \to 0$	Depends on q-distribution in the range $0.04 \lesssim q \lesssim 0.1$; flatter distributions give lower birthrates	Not relevant
Fraction of systems with $P_X < 20\ h$[a]	Increases slowly as α_{CE} decreases from 1.0 to 0.3, and increases rapidly for $\alpha_{CE} \lesssim 0.3$	Vanishes for $\langle V_k^2 \rangle^{1/2} \lesssim 100$ km s^{-1}; asymptotically approaches 0.75 for $\langle V_k^2 \rangle^{1/2} \gtrsim 400$ km s^{-1}	Very insensitive	Not relevant
Fraction of NS accretors[b]	Insensitive	Insensitive	Insensitive	>0.4 only for $M_{NS}^{max} > 1.95\ M_\odot$
Systemic velocity dispersion[a]	Varies as $\alpha_{CE}^{-1/4}$	Varies as $\langle V_k^2 \rangle^{1/5}$, and flattens at ~ 400 km s^{-1} for $\langle V_k^2 \rangle^{1/2} > 500$ km s^{-1}	Insensitive	Not relevant

[a] Total, sub- (S_E) plus super-Eddington (S^E), LMXB population.
[b] Sub-Eddington (S_E) LMXB population only.

twice the presupernova separation (Kalogera 1996), small values of α_{CE} also suppress the long-period extreme in this distribution (see Fig. 10). The slow increase in systemic velocity dispersion of survivors as α_{CE} decreases reflects (1) the selection of survivor systems, crudely, according to whether the supernova kick by chance imparts to the neutron star a space velocity closely matching the orbital velocity its companion at the instant of the explosion, and (2) the closing of the window in separation spanned by companion stars of different masses.

Average kick velocity.—The dynamical consequences of supernova kicks are described in some detail by Kalogera (1996). Aside from a nearly uniform suppression of survival probabilities, rms kick velocities exceeding the largest presupernova relative orbital velocities (~ 300 km s^{-1}) exercise very little influence either on the mass and orbital period distribution of survivors or on their space velocities, since survivors then come only from the low-velocity tail of the Maxwellian kick distribution. However, when kick velocities are small, they are capable only of binding relatively wide systems, which have correspondingly small presupernova relative orbital velocities, and consequently acquire only small postsupernova space velocities. (These wide systems survive common envelope evolution only if $\alpha_{CE} \gtrsim 0.5$.) Small kick velocities therefore suppress birthrates (Fig. 11), most severely among short-period systems (Fig. 12).

Mass ratio distribution.—As noted above, the range in primary masses ($\sim$15–25 $M_\odot$), secondary masses ($\sim$0.5–1.5 $M_\odot$), and orbital periods ($\sim$2–5 yr) from which progenitor binaries are drawn (see Fig. 4) is far beyond exploration by current observational techniques. We consider that our adopted mass ratio distribution represents a plausible maximum frequency to such systems, consistent with constraints of dynamical stability. The birthrates we derive must therefore be considered upper limits. Alternative choices of mass ratio distribution produce lower birthrates; to the extent that they differ greatly in functional form within the mass ratio window of interest ($q \sim$ 0.04–0.1), they may also alter the character of the LMXB distribution with respect to structural parameters. For example, Figure 13 illustrates the period distribution

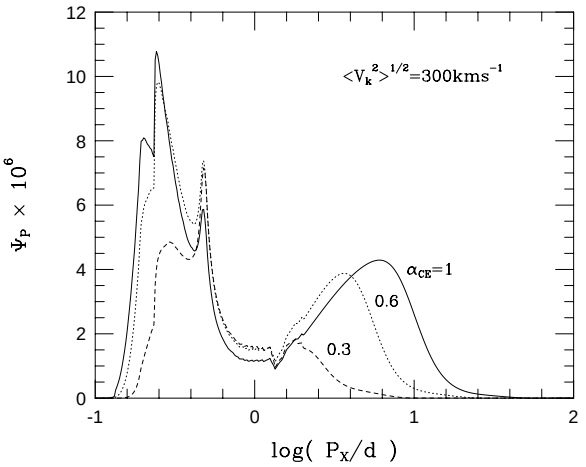

FIG. 10.—Distribution of systems, $\Psi_P(\log P_X)$, transferring mass at sub- and super-Eddington rates over orbital period, P_X, for different values of the common envelope efficiency, α_{CE}, and for $\langle V_k^2 \rangle^{1/2} = 300$ km s^{-1}.

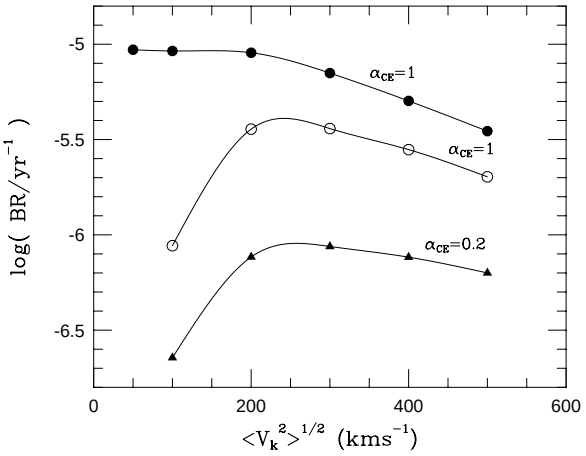

FIG. 11.—Total birthrate of sub-Eddington only (*open circles*) and sub- and super-Eddington combined (*filled circles*) nascent LMXBs for $\alpha_{CE} = 1$ and sub- and super-Eddington (*filled triangles*) systems for $\alpha_{CE} = 0.2$ as a function of $\langle V_k^2 \rangle^{1/2}$.

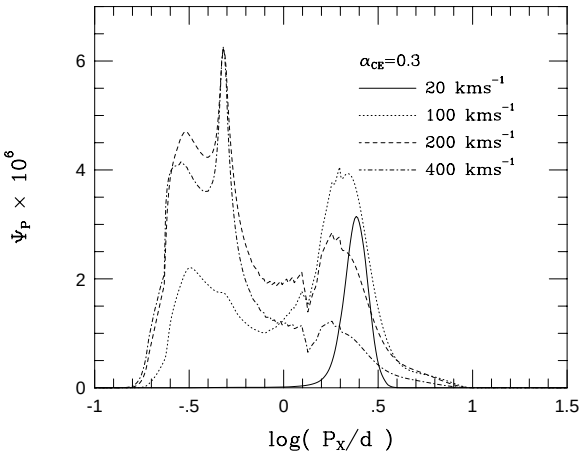

FIG. 12.—Distribution, $\Psi_P(\log P_X)$, of combined sub- and super-Eddington nascent LMXBs over orbital period, P_X, for different values of $\langle V_k^2 \rangle^{1/2}$ and for $\alpha_{CE} = 0.3$.

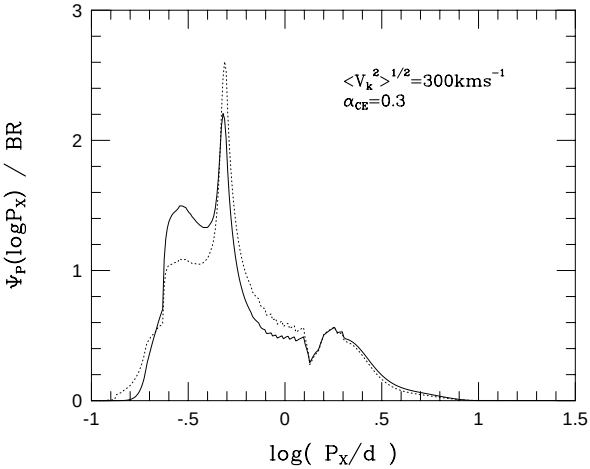

FIG. 13.—Distribution of systems, $\Psi_P(\log P_X)$, transferring mass at both sub- and super-Eddington rates over orbital period, P_X. The probability density is normalized to the total birthrate, 3.2×10^{-6} yr^{-1} for our reference model (*solid line*), and 1.2×10^{-7} yr^{-1} for a model with constant mass-ratio distribution (*dotted line*). For both cases $\langle V_k^2 \rangle^{1/2} = 300$ km s^{-1} and $\alpha_{CE} = 0.3$.

derived for a mass ratio distribution that is independent of q (apart from a very weak dependence introduced by retention of the Poisson cutoff parameter) below a critical mass ratio, $q_c = 0.35$. (Such a distribution closely resembles those used for example by Pols et al. 1991 and Dalton & Sarazin 1995.) In this case, the total birthrate decreases by a factor of $\simeq 27$, and there is a relative shift among surviving systems from the period range $0^d.2$–$0^d.5$ to the range $0^d.5$–1^d, a consequence of the flattening in mass ratio distribution in the range of interest, $q \sim 0.04$–1. For values of α_{CE} close to unity (not shown), a relative excess of short-period systems appears below $\sim 0^d.2$, but these systems do not survive common envelope evolution in our reference case. Unfortunately, these variations tend to be confined largely to the short-period ($P_X < 20$ hr) part of the orbital period distribution, where they are easily masked by secular evolution. The number ratio of long-period to short-period systems, which is the principal factor influencing systemic velocities as well, is only weakly dependent on the distribution of donor stars in mass (see Fig. 6), so long as most of those donors are massive enough ($\gtrsim 1.0\ M_\odot$) to evolve to interaction.

Maximum neutron star mass.—Given our observationally motivated assumption that neutron stars are born with uniform gravitational masses of 1.4 $M_\odot$, this factor enters only into the estimate of the fraction of LMXB accretors that may evolve to collapse to a black hole. Estimates of this fraction for a range of equations of state (Cook et al. 1994), along with the observational limit (Table 1), demand that the equation of state be relatively stiff and the maximum baryonic mass for neutron stars exceed $\sim 1.9\ M_\odot$.

7. CONCLUSIONS

On undertaking this study, we hoped that the population synthesis calculations described here would identify some feature or features among observable parameters of LMXBs that might be unique artifacts of their primordial distribution and of the evolutionary pathways leading to the LMXB state. The analytic technique we have used to execute our synthesis calculations offers enormous advantages for this purpose over Monte Carlo approaches, as it is free of statistical noise and can in principle yield arbitrarily high resolution in the distribution of final parameters (or of intermediate parameters), should it be warranted, at minimal additional computational cost. Our initial hopes have been confounded by the realization that supernova kicks must play a pivotal role in the formation of LMXBs, one which severely limits our ability to probe their origins on the basis of their observed properties. We see three important conclusions emerging from this study:

1. In the absence of supernova kicks, no LMXBs are formed at short ($P_X \lesssim 1^d$) orbital periods. Stellar winds from the helium star component during the post–common envelope, presupernova phase are capable of removing enough mass to reduce many presupernova systems to less than twice the mass of the postsupernova remnant (companion plus neutron star), a necessary condition for the binary condition to remain bound under instantaneous mass loss. However, short-period systems cannot then accommodate the much greater presupernova expansion of the low-mass helium star. Unless moderately large natal kicks are imparted to neutron stars (i.e., kicks averaging a substantial fraction of the relative orbital velocity of the binary at the supernova stage), only sufficiently long-period systems survive, and then only if α_{CE} is large ($\alpha_{CE} > 0.6$). These long-period systems all contain giant branch donors, and transfer mass at super-Eddington rates.

This conclusion in fact applies not only to the evolutionary channel explored here but to any putative formation channel in which the neutron star progenitor has a nondegenerate envelope. Stars with massive degenerate cores and hydrogen-rich envelopes, either in place of or in addition to helium envelopes, become red supergiants and could leave only extremely long-period neutron star binaries. Only accretion-induced collapse, in which the neutron star progenitor is virtually completely degenerate, could allow pre-SN systems close enough (and with little enough gravitational mass lost in the collapse) to produce short-period LMXBs in the absence of supernova kicks. However, whether accretion-induced collapse is a viable neutron star formation mechanism remains an unresolved issue: We are not aware of any plausible model that would feed accreted matter through a hydrogen-burning shell fast enough to stabilize helium burning (and thereby avoid mass loss during helium runaways) on a massive degenerate core; on the contrary, evolutionary models of luminous asymptotic giant branch stars invariably display thermally pulsing helium shells (Iben & Renzini 1983).

2. The characteristics of newborn LMXBs are almost entirely independent of the history of their progenitors. The ranges in donor masses and orbital periods allowed to LMXBs are dictated by age and stability constraints at the onset of the mass transfer phase. The distribution of systems over these parameters is influenced primarily by the efficiency of magnetic braking, which separates short- from long-period LMXBs. To a much smaller extent, it is also affected (1) by the average magnitude of the supernova kick, the effect being more evident when this average tends to very small values (i.e., disappearance of short-period LMXBs in the absence of kicks); and (2) by the common envelope efficiency, values of $\alpha_{CE} < 0.1$ precluding LMXB formation altogether. Apart from these extreme circumstances, supernova kicks obliterate any memory of how binaries arrived at the supernova stage; the LMXB distribution carries virtually no information about their evolutionary history. As a result, alternative formation mechanisms are indistinguishable, except where an evolutionary channel leads to pre-SN binaries dramatically different from those relevant to the present study, e.g., the direct-SN mechanism (Kalogera 1998). Common envelope evolution, which characterizes all other LMXB formation channels proposed to date, inevitably leads to similar distributions of short-period pre-SN binaries, sharing as their most prominent feature a short-period cutoff dictated by the dimensions of donor and pre-SN components.

3. Except as upper limits, theoretical estimates of galactic LMXB birthrates are not credible. These estimates depend one-for-one on the birth frequency of primordial binaries with suitable initial properties (in our case, $M_1 \sim 12$–$25\ M_\odot$, $M_2 \sim 0.5$–$2\ M_\odot$, and $P \sim 2$–5 yr ($A \sim 800$–$1800\ R_\odot$). While details may vary somewhat, all LMXB formation channels (including those proceeding through accretion-induced collapse) appeal to a primordial population of massive stars ($M_1 \gtrsim 10\ M_\odot$) with low-mass companions ($M_2 \lesssim 2\ M_\odot$) in long-period orbits ($P > 1$ yr). The true frequency of such systems is observationally indetermi-

nate and is constrained in the number density of low-mass companions a massive star may retain consistent with dynamical stability. In our case, we have pushed the binary frequency to this limit and so treat our birthrate estimates as upper limits. We have found, moreover, that even variations among possible mass ratio distributions within the range of interest are probably obscured in their effect on LMXB properties by secular evolution in that state.

Our conclusions regarding the role of supernova kicks in LMXB formation support and extend those reached independently by Terman et al. (1996; hereafter TTS96). In contrast, Iben et al. (1995; hereafter ITY95) found such kicks unnecessary. This difference appears to have its origin in several factors. One is the definition of common envelope efficiency. That which we use is identical with that employed by TTS96; as previously noted by Han, Podsiadlowski, & Eggleton (1995) and again by TTS96, the expression used by ITY95 understates the binding energy of the envelope by a factor of 2 or 3, whereas detailed numerical simulations presented by Rasio & Livio (1996) are consistent with our expression (eq. [A8]). ITY95 thus find wider post–common envelope systems, capable of accommodating the radial expansion of the helium star progenitors of neutron stars. Interestingly, in this regard, their models with assumed efficiency $\alpha_{CE} = 0.5$, corresponding roughly to our $\alpha_{CE} = 1$, produce no LMXBs with main-sequence donors (see Table 1 in ITY95), in agreement with our results. A second major difference concerns the extent and consequences of wind mass loss from helium stars. In contrast to our models and to TTS96, ITY95 find significant contributions to the total LMXB birthrate from systems undergoing case B mass transfer, which leave post–common envelope core-helium burning primaries. We find that the extensive mass loss suffered by helium stars during core helium burning (eq. [A9]) greatly expands the range of initial helium star masses and separations for which Roche lobe overflow will abort evolution prior to core collapse (see Fig. 2 and eq. [A10]), eliminating such stars as viable LMXB progenitors.

A final word is in order regarding angular momentum loss rates due to magnetic braking. We have not explored the dependence of our results on variants of our adopted braking rate. Qualitatively, stronger braking will enable wider postsupernova systems to form short-period LMXBs. For example, King & Kolb (1997) were able to produce short-period LMXBs with donors more massive than 1.3 $M_\odot$ without invoking kicks (these are not included by ITY95 or TTS96), because they assume a magnetic braking law stronger than ours by about an order of magnitude. However, our interpretation of braking rates among single stars indicates that magnetic braking is strongly suppressed at masses this large (see eq. [9]).

It is a pleasure to thank an anonymous referee for comments that helped us improve the focus of our paper. We are grateful to D. Psaltis for numerous valuable discussions and for carefully reading the manuscript. We also thank I. Iben, A. V. Tutukov, and L. R. Yungel'son for stimulating and enlightening discussions and for their help in identifying the root causes for differences in our results; and U. Kolb for help in resolving the effect of the efficiency of magnetic braking. This work was supported by National Science Foundation under grant AST 92-18074 and the Graduate College of the University of Illinois under a Dissertation Completion Fellowship.

APPENDIX

ANALYTIC APPROXIMATIONS USED IN THE MODEL

Following are the basic analytic relationships employed in our population synthesis models for the formation of LMXBs. They are grouped in roughly the sequence in which they enter consideration along the evolutionary path from primordial binary to ZALMXB. References identify the sources of the relationships used here, or (for stellar models) the detailed calculations which we here analytically approximate. The stellar models in each case assumed solar composition. The units used throughout are *masses* (M) in $M_\odot$; *radii* (R) and *orbital separations* (A) in $R_\odot$; *orbital periods* (P) in days; *orbital angular frequencies* (ω) in Hz; and *evolutionary times* (t) in years. Natural logarithms are written "ln," decimal logarithms "log," and arguments of trigonometric functions are in radians.

Massive stars (Schaller et al. 1992; Woosley & Weaver 1986).—Total stellar mass, reduced by stellar wind losses, of a star at core helium ignition, $M_{1,i}$, and at core helium exhaustion $M_{1,e}$, as a function of its initial mass, $10\ M_\odot < M_{1,0} < 40\ M_\odot$:

$$\log M_{1,i} = 0.9454 \log M_{1,0} + 0.0533 \tag{A1}$$

$$\log M_{1,e} = 0.81 \log M_{1,0} + 0.174 \quad M_{1,0} \leq 20\ M_\odot$$

$$= \tfrac{1}{2}[(0.81 \log M_{1,0} + 0.174)(1 - \sin\phi) + 0.9095(1 + \sin\phi)] \qquad 20\ M_\odot < M_{1,0} < 40\ M_\odot\ , \tag{A2}$$

where $\phi = 10[\log M_{1,0} - \log(20) - \pi/20]$. Mass of the helium core, M_{He}, produced by a star of initial mass $M_{1,0}$ *before* central He ignition:

$$\log M_{He} = 1.589 \log M_{1,0} - 1.393\ . \tag{A3}$$

If the massive star evolves through the core He burning phase, the He-core mass grows in mass by $\simeq 1.1\ M_\odot$ because of shell-hydrogen burning. The helium core is subsequently exposed by common envelope evolution, becoming the primary component mass in the next evolutionary phase.

Radii of stars at core helium ignition, $R_{1,i}$, at core helium exhaustion, $R_{1,e}$, and at core collapse, $R_{1,\mathrm{SN}}$:

$$\log R_{1,i} = 1.0785 \log M_{1,0} + 1.5123\ M_{1,0} \leq 20\ M_\odot$$
$$= \tfrac{1}{2}[(1.0785 \log M_{1,0} + 1.5123)(1 - \sin\phi) + (1.053 \log M_{1,0} + 1.111)(1 + \sin\phi)] \qquad 20\ M_\odot < M_{1,0} < 40\ M_\odot\ , \tag{A4}$$

where $\phi = 15[\log M_{1,0} - \log(20) - \pi/30]$,

$$\log R_{1,e} = 1.5745 \log M_{1,0} + 0.97125 \qquad M_{1,0} \leq 20\ M_\odot$$
$$= \tfrac{1}{2}[(1.5745 \log M_{1,0} + 0.97125)(1 - \sin\phi) + 0.74(1 + \sin\phi)] \qquad 20\ M_\odot < M_{1,0} < 40\ M_\odot\ , \tag{A5}$$

where $\phi = 12[\log M_{1,0} - \log(20) - \pi/24]$,

$$\log R_{1,\mathrm{SN}} = 1.148 \log M_{1,0} + 1.5888 \qquad M_{1,0} \leq 20\ M_\odot\ ,$$
$$= \tfrac{1}{2}\ [(1.148 \log M_{1,0} + 1.5888)(1 - \sin\phi) + 0.65(1 + \sin\phi)] \qquad 20\ M_\odot < M_{1,0} < 40\ M_\odot\ , \tag{A6}$$

where $\phi = 12[\ \log M_{1,0} - \log(20) - \pi/24]$.

Roche geometry (Eggleton 1983).—Dimensionless radius of the Roche lobe of component 1 ($r_{L_1} \equiv R_{L_1}/A$) as a function of binary mass ratio ($q_1 \equiv M_1/M_2$):

$$r_{L_1} = \frac{0.49 q_1^{2/3}}{0.6 q_1^{2/3} + \ln(1 + q_1^{1/3})}\ . \tag{A7}$$

Component indices are interchangeable in this expression.

Common envelope evolution (Webbink 1984).—Ratio of post–common envelope binary separation, A_f, to pre–common envelope separation, A_i:

$$\frac{A_f}{A_i} = \frac{\alpha_{\mathrm{CE}} r_{L_1}}{2}\left(\frac{M_2}{M_1}\right)\left[\frac{M_{\mathrm{He}}}{(M_1 - M_{\mathrm{He}}) + (1/2)\alpha_{\mathrm{CE}} r_{L_1} M_2}\right]. \tag{A8}$$

Helium stars (Habets 1985; Woosley et al. 1995).—Helium stars experience mass loss in a wind and their masses can decrease significantly during the central-He burning phase. The final mass of a helium star, $M_{\mathrm{He},f}$, at supernova as a function of its mass, M_{He} at core helium ignition is approximated by

$$M_{\mathrm{He},f} = 3.64 - 6.42 \exp\left[-\frac{(M_{\mathrm{He}} - 3.43)^{0.33}}{0.55}\right] \qquad 4M_\odot < M_{\mathrm{He}} < 20\ M_\odot. \tag{A9}$$

If the helium star is exposed after central He exhaustion, then it is not affected by mass loss and its mass at supernova is equal to its mass at the end of the time of its exposure. Radius of helium star at supernova, $R_{\mathrm{He},f}$:

$$R_{\mathrm{He},f} = 3.0965 - 2.013 \log M_{\mathrm{He},f} \qquad M_{\mathrm{He},f} \leq 2.5\ M_\odot$$
$$= 0.0557[(\log M_{\mathrm{He},f} - 0.172)^{-2.5}] \qquad M_{\mathrm{He},f} > 2.5\ M_\odot\ . \tag{A10}$$

Angular momentum loss.—Loss rate from gravitational radiation for a circular orbit (Landau & Lifshitz 1951):

$$\dot{J}_{\mathrm{GR}} = -\frac{32}{5}\frac{G}{c^5}\left(\frac{M_{\mathrm{NS}} M_2}{M_{\mathrm{NS}} + M_2}\right)^2 A^4 \omega^5\ , \tag{A11}$$

where G is the gravitational constant, c is the speed of light, and ω is the orbital frequency. We neglect the enhancement of gravitational radiation losses in eccentric orbits (Peters & Mathews 1963). The above equation can be integrated over a time interval Δt required for a circular orbit to decay from orbital period P_i to P_f:

$$P_f^{8/3} - P_i^{8/3} + 8A_{\mathrm{GR}}\Delta t = 0\ , \tag{A12}$$

where

$$A_{\mathrm{GR}} = \frac{q(1 + q)^{-1/3} M_{\mathrm{NS}}^{5/3}}{3.75 \times 10^{11}}\ \mathrm{yr}^{-1}\ \mathrm{day}^{8/3} \qquad q = \frac{M_2}{M_{\mathrm{NS}}}\ .$$

Loss rate from the magnetic stellar wind of a synchronously rotating secondary (see Rappaport et al. 1983):

$$\dot{J}_{\mathrm{MB}} = -1.8 \times 10^{47} b(M_2) M_2 R_2^2 \omega^3\ , \tag{A13}$$

where $\dot{J}_{\rm MB}$ is in cgs units (dyn cm s^{-1}) and $b(M_2)$ is the magnetic braking efficiency (eq. [9]), which becomes equal to zero for fully convective stars ($M_2 \leq 0.37\ M_\odot$). For stars with radiative cores ($M_2 > 0.37\ M_\odot$), we neglect the evolutionary expansion of the secondary with time and find that during a time interval Δt a circular orbit decays from orbital period P_i to P_f:

$$\frac{a}{4}(P_f^{8/3} - P_i^{8/3}) - \frac{a^2}{3}(P_f^2 - P_i^2) + \frac{a^3}{2}(P_f^{4/3} - P_i^{4/3}) - a^4(P_f^{2/3} - P_i^{2/3}) + a^5 \ln \frac{1 + P_f^{2/3}/a}{1 + P_i^{2/3}/a} + 2A_{\rm MB}\,\Delta t = 0\ , \qquad \text{(A14)}$$

where

$$A_{\rm MB} = b(M_2)\,\frac{q^2(1+q)^{1/3}M_{\rm NS}^{4/3}}{5.78 \times 10^9}\ {\rm yr}^{-1}\ {\rm day}^{10/3}\ , \qquad a = \frac{A_{\rm MB}}{A_{\rm GR}}\ .$$

Low-mass stars.—Radii at ZAMS, terminal main sequence, and at the base of the giant branch, along with the time evolution of the stellar radius have been given in Paper I.

REFERENCES

Abt, H. A. 1983, ARA&A, 21, 343
Allen, C. W. 1973, Astrophysical Quantities (London: Athlone)
Bailes, M. 1989, ApJ, 342, 917
Bailyn, C. D., Orosz, J. A., McClintock, J. E., & Remillard, R. A. 1995, Nature, 378, 157
Bhattacharya, D., & van den Heuvel, E. P. J. 1991, Phys. Rep., 203, 1
Boersma, J. 1961, Bull. Astron. Inst. Netherlands, 505, 291
Bradt, H. V., & McClintock, J. E. 1983, ARA&A, 21, 13
Caraveo, P. A. 1993, ApJ, 415, L111
Charles, P. A., & Casares, J. 1995, IAUC 6193
Clemens, D. P. 1985, ApJ, 295, 422
Cook, G. B., Shapiro, S. L., & Teukolsky, S. A. 1994, ApJ, 424, 823
Cowley, A. P. 1994, in The Evolution of X-Ray Binaries, ed. S. S. Holt & C. S. Day (New York: AIP), 45
Dalton, W. W., & Sarazin, C. L. 1995, ApJ, 448, 369
Darwin, G. H. 1879, Philos. Trans. R. Soc. London, 170, 1–35, 447
de Kool, M. 1992, A&A, 261, 188
Dewey, R. J., & Cordes, J. M. 1987, ApJ, 321, 780
Duquennoy, A., & Mayor, M. 1991, A&A, 248, 485
Eggleton, P. P. 1983, ApJ, 268, 386
Eggleton, P. P., & Verbunt, F. 1986, MNRAS, 220, 13P
Frail, D. A., Goss, W. M., & Whiteoak, J. B. Z. 1994, ApJ, 437, 781
Fukuda, I. 1982, PASP, 94, 271
Habets, G. M. H. J. 1985, Ph.D. thesis, Univ. of Amsterdam
Han, Z., Podsiadlowski, P., & Eggleton, P. P. 1995, MNRAS, 270, 121
Harrington, R. S. 1975, ApJ, 80, 1081
Harrison, P. A., Lyne, A. G., & Anderson, B. 1993, MNRAS, 261, 113
Hjellming, M. S., & Taam, R. E. 1991, ApJ, 370, 709
Hogeveen, S. J. 1991, Ph. D. thesis, Univ. of Amsterdam
Iben, I., Jr., & Livio, M. 1993, PASP, 105, 1373
Iben, I., Jr., & Renzini, A. 1983, AR&A, 21, 271
Iben, I., Jr., Tutukov, A. V., & Yungel'son, L. R. 1995, ApJS, 100, 233 (ITY95)
Johnston, H. M. 1992, Ph.D. thesis, California Inst. of Technology
Kalogera, V. 1996, ApJ, 471, 352
———. 1998, ApJ, 493, 368
Kalogera, V., & Webbink, R. F. 1996, ApJ, 458, 301 (Paper I)
Kawaler, S. D. 1987, PASP, 99, 1322
King, A. R., & Kolb, U. 1997, ApJ, 481, 918
Kiseleva, L. G., Eggleton, P. P., & Anosova, J. P. 1994, MNRAS, 267, 161
Kolb, U. 1993, A&A, 271, 149
Landau, L., & Lifshitz, E. 1951, The Classical Theory of Fields (Cambridge: Addison-Wesley)
Lipunov, V. M., & Postnov, K. A. 1988, Ap&SS, 145, 1
Lyne, A. G., & Lorimer, D. R. 1994, Nature, 369, 127
Paczyński, B. 1971, AR&A, 9, 183
———. 1976, in IAU Symp. 73, Structure and Evolution of Close Binary Systems, ed. P. P. Eggleton, S. Milton, & J. Whelan (Dordrecht: Reidel), 75
Peters, P. C., & Mathews, J. 1963, Phys. Rev., 131, 435
Politano, M. J. 1996, ApJ, 465, 338
Pols, O. R., Coté, J., Waters, L. B. F. M., & Heise, J. 1991, A&A, 241, 419
Pylyser, E. H. P., & Savonije, G. J. 1989, A&A, 208, 52
Rappaport, S. A., Verbunt, F., & Joss, P. C. 1983, ApJ, 275, 713
Rasio, F. A., & Livio, M. 1996, ApJ, 471, 366
Remillard, R. A., Orosz, J. A., McClintock, J. E., & Bailyn, C. D. 1996, ApJ, 459, 226
Romani, R. W. 1992, ApJ, 399, 621
Scalo, J. M. 1986, Fundam. Cosmic Phys., 11, 1
Schaller, G., Schaerer, D., Meynet, G., & Maeder, A. 1992, A&AS, 269, 331
Taam, R. E., Flannery, B. P., & Faulkner, J. 1980, ApJ, 239, 1017
Terman, J. L., Taam, R. E., & Savage, C. O. 1996, MNRAS, 281, 552 (TTS96)
Tutukov, A. V., & Yungel'son, L. R. 1993, AZh, 70, 812
van den Heuvel, E. P. J. 1983, in Accretion-driven Stellar X-Ray Sources, ed. W. H. G. Lewin & E. P. J. van den Heuvel (Cambridge: Cambridge Univ. Press), 303
van Paradijs, J. 1995, in X-Ray Binaries, ed. W. H. G. Lewin, J. van Paradijs & E. P. J. van den Heuvel (Cambridge: Cambridge Univ. Press), 536
Verbunt, F. 1993, ARA&A, 31, 93
Verbunt, F., & Zwaan, C. 1981, A&A, 100, L7
Webbink, R. F. 1984, ApJ, 277, 355
Webbink, R. F., & Kalogera, V. 1994, in The Evolution of X-Ray Binaries, ed. S. S. Holt & C. S. Day (New York: AIP), 321
Webbink, R. F., Rappaport, S., & Savonije, G. J. 1983, ApJ, 270, 678
Whelan, J., & Iben, I., Jr. 1973, ApJ, 186, 1007
Wiringa, R. B., Fiks, V., & Fabrocini, A. 1988, Phys. Rev. C, 38, 1010
Woosley, S. E., Langer, N., & Weaver, T. A. 1995, ApJ, 448, 315
Woosley, S. E., & Weaver, T. A. 1986, ARA&A, 24, 205
Zahn, J.-P. 1977, A&A, 57, 383
———. 1989, A&A, 220, 112